

# Organic electronics for neuromorphic computing

Yoei van de Burgt<sup>1\*</sup>, Armantas Melianas<sup>2\*</sup>, Scott Tom Keene<sup>2</sup>, George Malliaras<sup>3</sup>  
and Alberto Salleo<sup>2</sup>

**Neuromorphic computing could address the inherent limitations of conventional silicon technology in dedicated machine learning applications. Recent work on silicon-based asynchronous spiking neural networks and large crossbar arrays of two-terminal memristive devices has led to the development of promising neuromorphic systems. However, delivering a compact and efficient parallel computing technology that is capable of embedding artificial neural networks in hardware remains a significant challenge. Organic electronic materials offer an attractive option for such systems and could provide biocompatible and relatively inexpensive neuromorphic devices with low-energy switching and excellent tunability. Here, we review the development of organic neuromorphic devices. We consider different resistance-switching mechanisms, which typically rely on electrochemical doping or charge trapping, and report approaches that enhance state retention and conductance tuning. We also discuss the challenges the field faces in implementing low-power neuromorphic computing, such as device downscaling and improving device speed. Finally, we highlight early demonstrations of device integration into arrays, and consider future directions and potential applications of this technology.**

Artificial intelligence and deep learning algorithms are increasingly important in many applications. While these algorithms resemble the workings of the human brain, they are traditionally implemented on a software level rather than emulated by hardware. Deep learning relies on artificial neural networks that are typically executed on computers based on the conventional von Neumann architecture, operating mostly sequentially. In contrast, the brain's hardware operates in a massively parallel fashion through a densely interconnected network of neurons. Communication between neurons is facilitated by chemical fluxes inside synapses that regulate the signal strength — or synaptic weight — that one neuron can pass to the next<sup>1</sup>. Neurons also follow the Hebbian learning principle: those that fire together, wire together<sup>2</sup>. This plasticity is thus thought to form the basis of learning and memory, and to be largely responsible for information processing inside the brain. A consequence of this architecture is that the brain is extremely energy-efficient compared with traditional computers, particularly for pattern recognition and classification tasks.

To execute neural network algorithms at an energy efficiency and interconnectivity comparable to that of the brain, it would thus be desirable to emulate synaptic functionality. Devices and circuits that possess the necessary characteristics were first described by Carver Mead in 1990, who coined the term 'neuromorphic electronic systems'<sup>3</sup>. As such, the idea of neuromorphic electronic systems has been around for decades, albeit with varying research attention.

On the one hand, asynchronous spiking neural networks based on silicon neurons and synapses, consisting of multi-element circuits<sup>4</sup>, have been the focus of attention in emulating large-scale biological neural networks, as well as in event-driven computing<sup>5</sup>. In these networks, information is encoded in spike timing and frequency<sup>6</sup>. Spiking networks have been utilized in some of the first commercial products, such as TrueNorth<sup>7</sup>, NeuroGrid<sup>8</sup> and Intel Loihi<sup>9</sup>.

On the other hand, following the seminal paper from Leon Chua, in which he theoretically described a memristor<sup>10</sup>, and then the first experimental demonstration of a memristor in 2008<sup>11</sup>, there has been a significant amount of research into facilitating

parallel computation, such as the development of analogue vector-matrix multiplication<sup>12</sup> by forward-inference neural networks<sup>6</sup>. In this case, each synaptic weight in an artificial neural network is emulated by a hardware-based tunable non-volatile resistive memory element (Box 1). In contrast with spiking neural networks, information is encoded solely in the resistance state of the non-volatile memory device.

Memristors, or more accurately memristive devices (the term 'memristor' is not always fully applicable<sup>10</sup>), are resistance switches that display a variable but non-volatile electrical resistance, depending on the history of applied voltage and current<sup>13</sup>. However, the concept of variable-resistance devices goes back to the late 1960s/1970s<sup>14,15</sup> and such devices have been demonstrated to display synaptic functionality resembling Hebbian learning<sup>16</sup>. These two-terminal memristive devices allow for the construction of networks that can be used not only as non-volatile memory arrays but also for processing information and carrying out simple pattern-recognition tasks directly in hardware, at relatively low energy cost<sup>17,18</sup>. The work of Strukov and colleagues has demonstrated that neural network algorithms, which traditionally have been implemented on a software level, could indeed be embedded in hardware itself, thus emulating the function and efficiency of the brain on a compact chip<sup>17,18</sup>.

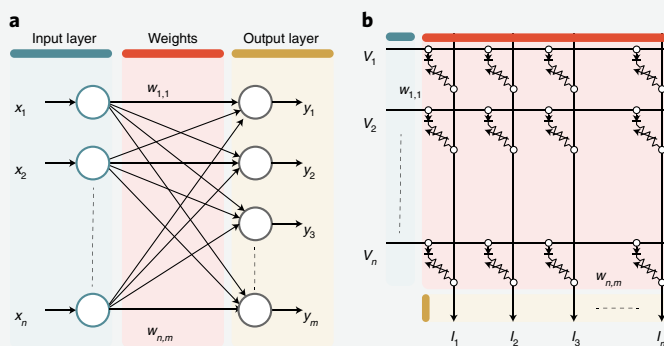
Although the use of an integrated network of memristive devices aims to emulate efficiently the parallel operation of the brain<sup>6</sup>, ideal neuromorphic devices intended for forward-inference neural networks should: operate with low energy (to reduce power consumption); have a large range of linearly and symmetrically programmable conductance states to facilitate 'blind' synaptic weight update during learning; and efficiently perform parallel vector-matrix multiplication. Requirements on state-retention time (a measure of how well a device can keep its state) can vary significantly depending on the application, but generally longer state-retention times are favoured; for example, for continuous learning the synaptic weights can be routinely offloaded to an external memory, whereas for train-once inference-only applications the weights are stored long-term on-chip.

<sup>1</sup>Microsystems and Institute for Complex Molecular Systems, Eindhoven University of Technology, Eindhoven, The Netherlands. <sup>2</sup>Department of Materials Science and Engineering, Stanford University, Stanford, CA, USA. <sup>3</sup>Electrical Engineering Division, Department of Engineering, University of Cambridge, Cambridge, UK. \*e-mail: [y.b.v.d.burgt@tue.nl](mailto:y.b.v.d.burgt@tue.nl); [armantas.melianas@stanford.edu](mailto:armantas.melianas@stanford.edu)

**Box 1 | Vector-matrix multiplication and learning can be efficiently emulated using hardware-based artificial neural networks**

Artificial neural networks connect an input layer (for example, pixels in an image or a list of data) to an output layer using hidden layers (see image). Each node is connected to the nodes of the next layer and as such these networks rely on the multiplication of large matrices and vectors for inference (that is, prediction) as well as learning. Connections between the nodes (synaptic weights) can be modulated to train the network to perform the desired operation. Vector-matrix multiplication — the basis of artificial neural network algorithms, including convolutional neural networks<sup>115</sup>, deep belief networks<sup>116</sup> and multilayer perceptrons<sup>117</sup> — can be efficiently implemented in hardware, for example in a crossbar array using analogue resistive memory elements<sup>6</sup> (indicated here by a variable resistor), by making use of Ohm's law and Kirchhoff's law. More concretely, vector-matrix multiplication performed in software  $y_m = \sum_n w_{n,m} x_n$  (figure panel a) is emulated via current-voltage operations as  $I_m = \sum_n G_{n,m} V_n$ , where  $G_{n,m}$  is the conductance of the neuromorphic device at the  $n,m$  node,  $V_n$  is applied voltage at the  $n$  input, and  $I_m$  is the read-out current at the  $m$  output (figure panel b). To avoid device crosstalk, each neuromorphic device is typically paired with an access device<sup>75</sup>. Learning in

these networks generally relies on the backpropagation method, a supervised learning algorithm in which the synaptic weights are iteratively adjusted according to the gradient of the error function<sup>76</sup>. These have shown promise for efficiently emulating artificial neural networks in recent commercially significant domains such as deep learning<sup>118</sup>.



Furthermore, bio-inspired devices based on tunable memory elements may require emulating additional brain-like functionality such as spike-timing-dependent plasticity (STDP), spike-rate-dependent plasticity or short- and long-term potentiation<sup>19,20</sup>. As a result, detailed requirements of neuromorphic devices are highly dependent on the particular application, as well as on the specific neural network architecture. Nevertheless, for efficient operation of hardware-based neural networks, several metrics are desired<sup>13,21–23</sup>, as suggested for devices relying on organic electronic materials in Table 1.

Tunable organic electronic materials and devices can serve as highly attractive alternatives to conventional memristive devices in specific neuromorphic applications, particularly for online learning where the synaptic weights are learned on-chip to make real-time predictions (that is, inference). The specific nature of organic materials may offer novel and alternative switching mechanisms that are less stochastic while retaining low-energy operation and large dynamic range, thus enabling high training and inference accuracy.

Furthermore, organic electronic materials are generally inexpensive, can be integrated in low-cost manufacturing processes such as inkjet printing, and their chemical, electrical and mechanical properties can be tailored to the desired application by chemical synthesis<sup>24</sup>. As such, organic electronic materials have been recently utilized in a variety of neuromorphic device configurations and have also been proposed for biology-related applications, thereby potentially opening up a path towards efficient and adaptable brain-machine interfacing. In this Review, we discuss how organic electronic materials could meet some of the most important criteria required for neuromorphic computing: analogue conductance tuning through access to a large number of distinct conductance states while maintaining low power consumption. At the same time, we highlight the key remaining challenges, which include device reproducibility, integration with conventional electronics, and the absence of a fully scalable fabrication process.

**State-of-the-art organic neuromorphic devices**

Similar to their inorganic counterparts, organic memristive devices were traditionally developed for non-volatile memory applications and generally consist of a two-terminal metal–insulator–metal configuration that demonstrates two stable, switchable conductance states<sup>25–30</sup>. Different configurations and active materials such as

polymers<sup>31</sup>, small molecules<sup>32</sup> and donor–acceptor complexes<sup>27,28</sup>, as well as ferroelectric materials<sup>33,34</sup>, have been proposed. In general, resistance switching in organic electronic materials is achieved by similar mechanisms as in inorganic materials, such as localized (for example, filamentary) conduction, ionic charge transfer and electromigration<sup>27,30,35</sup> (Fig. 1). Most of these materials and devices, as well as their switching mechanisms, have been extensively described in other review articles<sup>36–39</sup>. Although binary (two-state) memory devices for neuromorphic computing have been demonstrated<sup>4,40</sup>, here we will focus mainly on organic memristive devices enabling continuous (that is, analogue) resistance tuning, which is ideally suited for on-chip learning and inference using parallel multiply–accumulate operations<sup>6,41</sup> and has also been proposed in a related inorganic system<sup>42</sup>. At the same time, the resemblance of specific organic memristive devices with biological synapses (for example, the coupling of ionic and electronic currents) constitutes signifi-

**Table 1 | Desired and recommended metrics for organic neuromorphic devices**

Parameter	Value
Size for integration	<1 $\mu\text{m}^2$ for dense/compact arrays
Number of states	~100 separable states, or ~6 bit
Conductance tuning	Linear and symmetric
Switching noise	<0.5% of weight range
Switching energy	<1 pJ per switching event
Write/read speed	<1 $\mu\text{s}$
State retention <sup>a</sup>	10 <sup>3</sup> –10 <sup>8</sup> s
Write endurance (cycles) <sup>b</sup>	~10 <sup>9</sup> (online learning)
Temperature stability <sup>c</sup>	Array operating temperature

<sup>a</sup>Long state retention is essential for hardware-based neural network inference using non-volatile memory elements (such as a dot-product engine<sup>43</sup>) but is not as critical for online learning, where synaptic weight values can be stored elsewhere after training. <sup>b</sup>High write endurance is more important for online learning than inference-only approaches, whose requirements on write endurance are less strict. <sup>c</sup>Device temperature stability is important to consider because neuromorphic arrays may heat up significantly during array operation. The relevant temperature range depends on the materials and system-level architecture. Note that device integration into inorganic/organic 3D stacks may require material stability at elevated processing temperatures, such as 350–400 °C for 'back end of the line' processing.

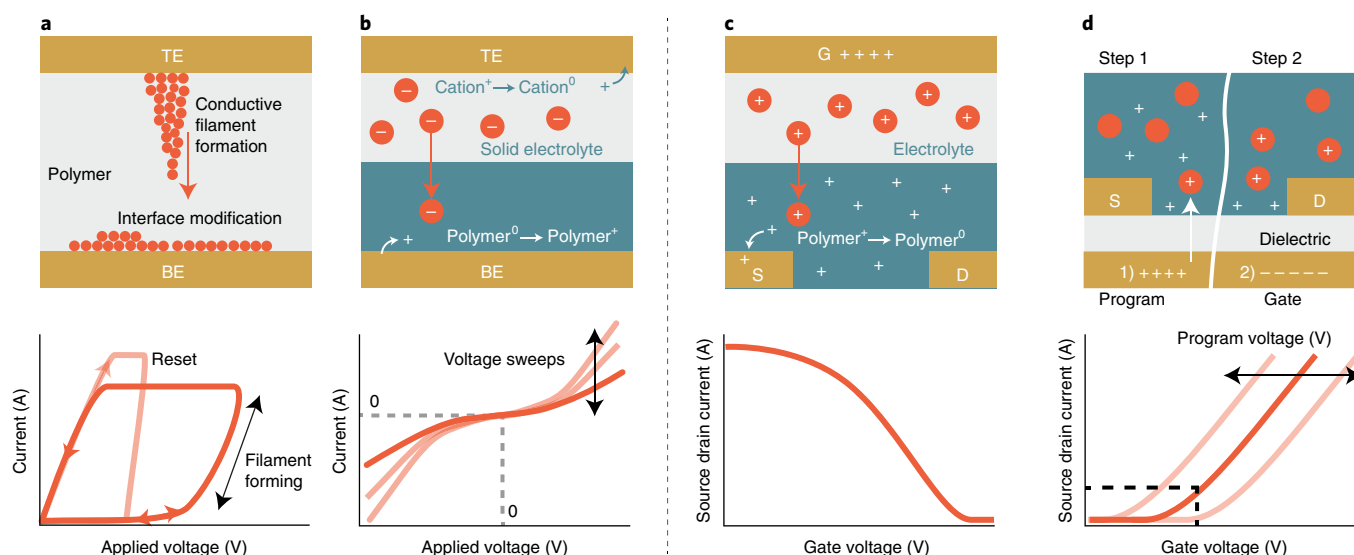


**Fig. 1 | Overview of conductance switching mechanisms in organic electronic materials.** **a**, Two-terminal organic memory based on localized conductive filament (or other conductive pathways) formation and/or bias-dependent interface modification. The bottom graph shows the current-voltage curve for a filament-forming device. TE, top electrode; BE, bottom electrode. **b**, Two-terminal redox-based switching with a counter-redox reaction. Upon applied potential, a redox reaction occurs in both the solid electrolyte as well as the polymer, which results in a modified conductance. **c**, Organic electrochemical redox-based switching. An applied potential on the gate drives ions from the electrolyte into the polymer, changing its redox state and conductivity as a result. G, gate; S, source; D, drain. **d**, Charge-trapping based switching. In Step 1 (programming) a high potential moves charges onto the nanoparticles in the film. In Step 2 (operation) a lower potential on the gate is used to open the channel. The amount of charges in the film determines the turn-on potential.

cance, particularly for emulating biological neural network behaviour using artificial synapses, which we also briefly describe here.

In addition, the specific requirements for memory applications differ from those relevant to neuromorphic computing. More concretely, while both applications require relatively high switching speeds and cycling endurance, state-retention time requirements are much more stringent for memory applications than for neuromorphic computing (Table 1), which is highlighted by the long state-retention of 'write-once-read-many times' devices<sup>43</sup>. On the other hand, it is essential for neuromorphic devices to display a large range of separable conductance states to perform neural network operations efficiently<sup>6,22</sup>. The unique conductance-tuning mechanisms of a range of organic electronic materials and devices have been exploited to demonstrate a variety of neuromorphic devices. Resistance switching in most devices relies on either electrochemical doping or charge-trapping, as summarized in Table 2 and schematically depicted in Fig. 1.

**Electrolyte-gated redox-based switching.** Most prominently, potentiation and depression effects are achieved by means of a gate electrode to tune the device's conductance gradually via electrochemical doping (Fig. 1b,c). This process can be achieved using an electrolyte (liquid or solid) that injects or extracts ions from the organic film, thus changing the doping (redox) state of the latter. In 1991, Kaneto et al. demonstrated a device in which two different currents, electronic and ionic, flow in perpendicular directions. This concept was utilized to tune the conductivity of an organic material with a solid electrolyte over three orders of magnitude<sup>44</sup>. Later, the work of Berggren<sup>45</sup> and Fontana<sup>46</sup> demonstrated liquid-electrolyte-based devices in which two stable conductance states were achieved with a large on/off ratio between the low and high conductance states ( $10^5$  in ref. <sup>45</sup> and  $\sim 10^2$  in ref. <sup>46</sup>). A similar configuration with an electrolyte-gated conducting polymer was used to display a range of neuromorphic functions<sup>47</sup>, while other polymeric materials, electrolytes<sup>48–50</sup> and nanowires<sup>51</sup> have also been

reported. Although typically these devices display only low- and high-conductance states, in some cases one of these states can be modulated in a continuous fashion by varying the gate potential or pulse frequency, thus enabling more than two conductance states (Table 2, Fig. 2a,b).

More recently, researchers demonstrated a modification of an organic electrochemical transistor-based system that comprised a conducting polymeric gate in combination with a de-doped conducting polymer channel<sup>52</sup>; that is, a device architecture reminiscent of an organic battery in which a counter-redox reaction in the gate ensures electrical neutrality throughout the device, resulting in enhanced state-retention. Similar battery-like devices have also been demonstrated using different polymers and solid electrolytes<sup>48,53</sup> and in a two-terminal configuration<sup>54</sup>, however, these devices were lacking an ionic-conductor separation layer between the two electrodes to prevent recombination reactions, thus causing undesirable self-discharge and limited state-retention.

Overall, the easily tailored characteristics and large tunable conductance range reported in a variety of electrolyte-gated organic materials and configurations have thus far shown great promise for neuromorphic computing applications.

**Charge-trapping-based switching.** Vuillaume and colleagues<sup>55</sup>, following previously reported bi-stable two-terminal organic memory research<sup>56,57</sup>, developed another widely used mechanism for displaying a memory effect and neuromorphic functionality in organic field-effect transistors based on charge trapping. These devices rely on charge storage on metallic (for example, Au) or non-metallic (for example, ZnO)<sup>58</sup> nanoparticles that act as nanoscale capacitors embedded in an organic semiconductor such as pentacene or poly(methyl methacrylate) (Fig. 1d). The charged particles electrostatically repel the mobile holes in pentacene and thus effectively modify the source-drain behaviour, enabling resistance tuning.

Since the nanoparticles reside inside the bulk of the material rather than in a separate layer, the mechanism differs from

**Table 2 | Switching mechanisms and materials used in organic neuromorphic devices**

Principle	Material / electrolyte	Number of states / tuning <sup>a</sup>	Memory mechanism	State retention <sup>b</sup> / demonstrated cycles <sup>c</sup>	Reference
Electrochemical doping	poly(3-methyl thiophene) / poly(ethylene oxide-propylene oxide) + LiClO <sub>4</sub>	4 / continuous	Counter-redox reaction + separation read/write	~hours / -	44
	PANI / PEO	>2	Slow kinetics	- / 10 <sup>4</sup> (ref. 87)	46,70,87,88,114
	MEH-PPV / RbAg <sub>4</sub> I <sub>5</sub>	8 / continuous	Diffusion disparity	~20 ms for STP and >240 h for LTP / -	67
	PQT / PEO + EV(ClO <sub>4</sub> ) <sub>2</sub>	2	Counter-redox reaction + separation read/write	14 h <sup>d</sup> (ref. 53) / > 100 (ref. 48)	48,53
	PEDOT:PSS / NaCl	>2	Slow kinetics	<1 s / -	47
	PEDOT:PTHF / NaCl	Continuous	Slow kinetics + structural rearrangement of the polymer	<1 s / -	68
	BTPA-F / PEO + EV(ClO <sub>4</sub> ) <sub>2</sub>	Continuous	Counter-redox reaction	~seconds / -	54
	P3HT / P(VDF-HFP) P3HT / P(VDF-TrFE)	>2	Slow kinetics	<10 s (ref. 50) / -	49,50
	P3HT / PEO	Continuous	Slow kinetics	<5 s / 60	51
	PEDOT:PSS / NaCl PEDOT:PSS / Nafion	512 / continuous	Counter-redox reaction + separation read/write	100 s / >15	52
Charge trapping	Pentacene (Au)	Continuous	Charge trapping nanoparticles	24 h / 800 (ref. 66)	55,61,62,66
	DNTT (Al)	Continuous	Charge trapping nanosheet	~1 s / -	60
Ion migration	Ti/PEDOT:PSS/TiAg/PEDOT:PSS/Ta	Continuous	Compound formation	~seconds (ref. 78) / -	78,72
Light-assisted reaction	P3HT / diarylethene	256	Energy level modification	>500 days / 70	73

<sup>a</sup>The number of demonstrated conductance states is given if mentioned in the original work. Some devices display both a low and a high conductance state, where one of the two can be modulated in a continuous fashion by varying the gate potential or pulse frequency (marked here as >2). <sup>b</sup>State-retention strongly depends on the number of defined states and the state from which the device is discharging. <sup>c</sup>Cycling until device failure (endurance) has not yet been demonstrated for most organic neuromorphic devices. The numbers cited here represent the minimum number of cycles during which the device was operating successfully. <sup>d</sup>Although the two conductance states were distinguishable during 14 hours of operation, the conductance of both states (on/off) decreased by several orders of magnitude. LiClO<sub>4</sub>, Lithium perchlorate; PANI, polyaniline; PEO, polyethylene oxide; MEH-PPV, poly[2-methoxy-5-(20-ethylhexyloxy)-p-phenylene vinylene]; PQT, poly(3,3'-didodecylquaterthiophene); EV(ClO<sub>4</sub>)<sub>2</sub>, ethyl viologen diperchlorate; PEDOT:PSS, poly(3,4-ethylenedioxythiophene) polystyrene sulfonate; NaCl, sodium chloride; PEDOT:PTHF, poly(3,4-ethylenedioxythiophene); poly(tetrahydrofuran); BTPA-F, triphenylamine-containing polymer; P3HT, poly(3-hexylthiophene); P(VDF-HFP), poly(vinylidene fluoride-co-hexafluoropropylene); P(VDF-TrFE), poly(vinylidene fluoride-co-trifluoroethylene); DNTT, dinaphtho[2,3-b:2',3'-f]thieno[3,2-b]thiophene.

conventional floating-gate transistors and related floating-gate organic memory devices<sup>59,60</sup>. Nevertheless, the channel must still be switched on by a gate potential to perform a read operation<sup>61</sup>. This requirement was removed by connecting the gate with the drain to form a pseudo-two-terminal configuration (requiring only a source-drain voltage), thus enabling the channel conductance to be modified as a function of the frequency of applied pulses<sup>62</sup>.

Organic memory transistors based on charge-trapping are promising, especially since they offer relatively large channel resistance — desirable for low power computing — and long state-retention times (~10<sup>5</sup> s). However, small channels can fit only a limited number of nanoparticles, which may limit device performance in dense device arrays. It remains to be seen whether these devices can be scaled down while retaining sufficiently low operating noise and device reproducibility.

### Opportunities and challenges for organic devices

As demonstrated by the successful large-scale commercialization of organic light-emitting diodes and initial attempts to commercialize organic photovoltaics, organic materials span a wide spectrum of properties that could be advantageous for neuromorphic computing applications, such as their excellent ability to be tailored, chemically, mechanically and electrically, to specific requirements. These qualities were recognized early on and have led to a wide variety of unique demonstrations of organic memories and organic neuromorphic devices. Most prominently, the ability for the conductance to be tuned, combined with the low energies required to do so, make organic materials particularly suitable for neuromorphic

applications. However, at the same time, the nature of these materials introduces challenges, specifically regarding materials and device stability, integration into arrays and device-to-device variability. Some of these challenges have recently been addressed in the literature but several remain, as the field of organic neuromorphic computing is steadily growing<sup>63</sup>.

**Number of conductance states.** Conventional organic and inorganic memristive devices often display only one low- conductivity state and one high-conductivity state. Several memristive devices, such as phase change materials<sup>64</sup>, vacancy migration-based materials and conductive filament-based devices have been shown to display more programmable states<sup>21</sup>, but are often stochastic and lack predictability, for example by displaying high write noise. Biological synapses, on the other hand, can change their conductance — or synaptic weight — in a virtually analogue fashion. In fact, hardware-implemented forward-inference neural networks generally require some form of analogue variation in the synaptic elements<sup>65</sup>, while a large tunable conductance range enhances artificial neural network accuracy and enables analogue computing<sup>22</sup>.

The first demonstrations of organic neuromorphic devices with a large number of conductance states were based on tuning the amount of charge on the gold nanoparticles dispersed throughout the bulk of a transistor channel<sup>55,61</sup> (Fig. 1d). Because the charged nanoparticles repelled mobile charge carriers inside the film, it was possible to tune the channel conductance accurately, with an on/off ratio of about 10<sup>3</sup>–10<sup>4</sup> (ref. 66). Similar to multi-level floating-gate memory, the charging of a gate electrode that was separated from



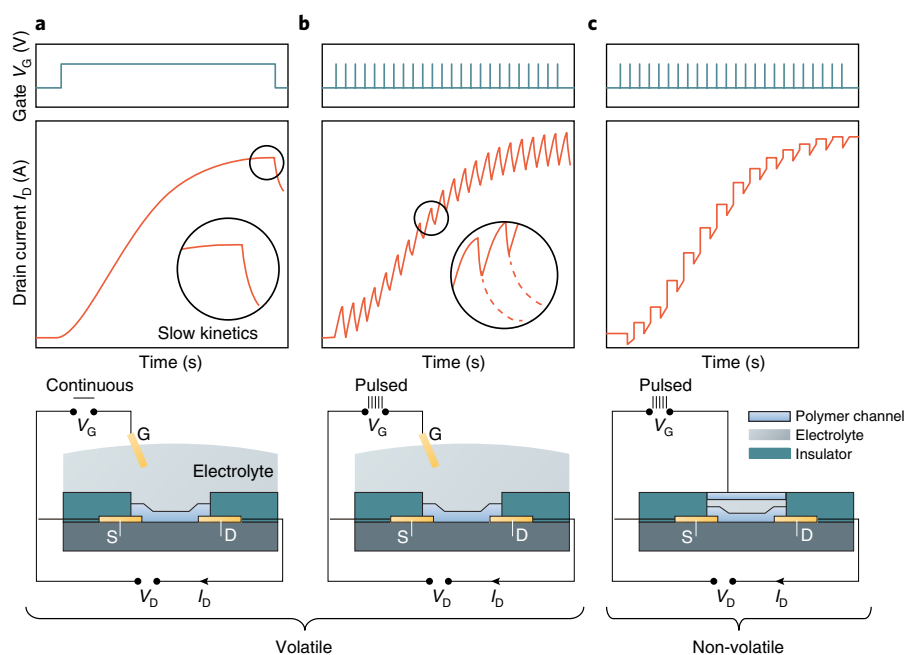


**Fig. 2 | Conductance tuning methods for electrolyte-gated redox-based neuromorphic devices.** **a**, A continuous gate gradually modifies the conductance, which returns to its original state upon removing the gate potential. **b**, Pulse train. Short pulses similar to that in **a** result in the gradual modification of the conductance. Upon stopping the pulses the conductance returns to its original state. **c**, Pulse train with polymeric electrode gate and decoupling of read and write operations. As a result of the decoupling of read and write operations, the achieved conductance state remains when the gate pulses end. Representations of the respective electrochemical devices are shown below the graphs. Credit: reproduced from ref. <sup>84</sup>, Springer Nature Ltd.

the channel also induced multi-level storage in organic memristive devices, although the corresponding write voltages were relatively high ( $\sim 40$  V)<sup>59</sup>.

Most electrolyte-based redox coupling mechanisms have displayed a gate-potential-dependent tuning of the channel conductance<sup>46,50,67–69</sup> (Fig. 2a) or demonstrated that a train of pulses could potentiate or depress the channel<sup>47,49,50,70,68</sup> (Fig. 2b). These tuning mechanisms rely on the change in the redox state of the polymer due to the electrochemical potential induced by the gate electrode. Changing this redox state results in a reduction or enhancement of the conductivity by decreasing or increasing the number of mobile charge carriers, respectively. At the same time, ions or other charge carriers must compensate for the induced space-charge in the film. Due to the physical movement of these charges, the process can be controlled relatively well by varying the gate potential and pulse frequency, which in fact resembles the processes occurring in biological synapses. The final conductance in the channel is independent of whether modulation was achieved using a train of short pulses or a continuous gate potential.

In contrast, a near-analogue tuning of channel conductivity was recently demonstrated by accurate protonic doping of a polyethylene-imine that in turn was used to de-dope the conducting polymer<sup>52</sup>. This device operation resembles that of an organic battery<sup>71</sup> in which both polymer electrodes are allowed to change their redox state during switching, thereby ensuring charge neutrality in both electrodes. In between read and write operations, the two electrodes are electrically isolated from each other to prevent charge exchange, thereby enhancing state-retention considerably — the device effectively operates as a non-volatile memory. As a result, it is possible to tune the conductance accurately through the complete set of redox states of the polymer (Fig. 2c), which somewhat resembles conductivity modulation by the p- or n-type doping of silicon.

While two-terminal devices commonly comprise organic memories that display only two conductance states, a few examples of multi-state devices also exist. For instance, a redox coupling

mechanism created a gradual change in conductance by consecutive voltage stimulations<sup>54</sup>, while a more traditional metal-polymer-metal configuration succeeded in displaying 100 conductance states<sup>72</sup>. In the latter, the authors used a Ti:PEDOT:PSS:Ti sandwich structure in which the interface between metal and conducting polymer was modified by the growth and migration of a Ti-compound, to display a gradual change in conductance. Although these two-terminal-based concepts benefit from possible smaller sizes and more straightforward operation and integration into a crossbar array, effective utilization of this concept would rely on significantly decreasing the write noise during the predominantly stochastic switching.

Finally, a more exotic multi-state organic memory device was demonstrated based on optically modifying the charge transport inside a poly(3-hexylthiophene) (P3HT) film blended with photochromic diarylethene<sup>73</sup>. Using ultraviolet and green light irradiation, the researchers were able to modulate the energy levels of the photochromic material inside the polymer matrix. Modifying the highest occupied molecular orbital levels towards that of P3HT results in better charge transport. As such, the researchers were able to accurately tune the device to 256 distinguishable conductance states. This is an interesting concept for further development in neuromorphic applications, especially since light-assisted programming<sup>74</sup> could potentially overcome several limitations in electrical memristive-based crossbar arrays, such as unwanted (sneak) currents, without the need to introduce sophisticated access devices<sup>75</sup> that prevent cross-talk.

**Short-term plasticity.** In the brain, communication between neurons is inherently dynamic and occurs over different timescales, ranging from milliseconds to months<sup>1</sup>. Changes in communication strength depend on the history of synapse activity — known as synaptic plasticity. Short-term plasticity modulation facilitates a variety of computational functionality in the brain, while long-term plasticity effects are attributed to learning and memory<sup>2</sup>. Both of these functionalities

have been reported in organic devices, with distinctions that lie predominantly in the specific application that is targeted.

Short-term plasticity is mostly useful for mimicking synapses and displaying synaptic functionality such as STDP, spike-rate-dependent plasticity and short-to-long-term plasticity. Devices and technologies that aim to mimic these specific synaptic functions are generally called ‘artificial synapses’. Such devices, in addition to helping us understand processes and dynamics inside the brain, have been useful in spiking neural networks<sup>4,7</sup>. As with real synapses, artificial synapses display a conductance that is a function of the history of previous applied pulses. In some cases, a leaky integrate-and-fire element is included as an artificial neuron, which resembles biological neuron functionality by controlling which signals pass to the next neural network layer. This is achieved through the integration of input signals until a threshold is reached, followed by the neuron firing a signal<sup>4</sup>.

STDP facilitates the modulation of the signal strength between two neurons inside a synapse, and is thus widely regarded as one of the fundamental mechanisms in biological neural networks. This process is based on the temporal difference between pre- and post-synaptic pulses arriving at the synapse. The shorter the time difference between the pulses, the higher the modulation of the synaptic weight. In contrast with error backpropagation<sup>76</sup> (global learning rule, directly relevant to array operation), STDP is a local learning mechanism and thus far has been demonstrated mainly on the single-device level in charge-trapping devices<sup>62</sup>, electrolyte-gated three-terminal architectures<sup>54,67,77</sup> and two-terminal organic memristive devices<sup>72,78</sup>. Spike-rate-dependent plasticity, a metric closely related to STDP, correlates the modulation with the rate of pulses that arrive to the gate, and has also been demonstrated in several three-terminal configurations<sup>61,78,79</sup>. Finally, short-to-long-term plasticity can be described as the effect in which repeated stimulation will result in a long-term modulation of the conductance, compared with a short-term plasticity effect for a single stimulation<sup>80</sup>. This transition was also imitated in an organic neuromorphic device by the gradual modification of a polymer–silver interface<sup>78</sup> (Fig. 1a).

Research on artificial synapses continues to inspire developments in mimicking biological synapses, particularly for use in spiking neural networks and gaining a deeper understanding of biological neural networks. However, for efficient on-chip learning it is essential to develop a global learning architecture next to the local STDP learning rule, while simultaneously increasing state-retention times in organic neuromorphic devices; that is, it is essential to develop artificial synapse devices that display ‘long-term memory’.

**Long-term plasticity and state-retention.** Long state-retention times and enhanced stability are desirable for hardware-based artificial neural networks and related vector–matrix multiplication. In fact, long state-retention times were first reported during the development of non-volatile organic memories, where state stability is crucial for preventing data loss<sup>33,43,81</sup>. Specifically, ‘write-once-read-many times’ devices<sup>43</sup> have shown long retention times of up to 500 days<sup>82</sup>, but more recent examples of multilevel optical memories (500 days<sup>73</sup>) or solution-processed azo-aromatics memories (11 days<sup>83</sup>) have also been demonstrated. Neuromorphic devices based on electrochemical doping allow operation in a larger conductivity range with more states than organic memories. To use multi-level devices in hardware-based neuromorphic arrays effectively, it is essential to increase the state-retention. A variety of research papers have included some form of state-retention measurements (Table 2).

Conducting polymer-based organic electrochemical transistors generally operate in depletion mode<sup>84</sup>. This means that the channel is in a high conducting state until ions are introduced that cause the extraction of mobile holes and de-doping of the conjugated polymer backbone. When the gate voltage ( $V_{\text{bias}}$ ) is switched off,

these ions return to the electrolyte and the polymer is again doped (Fig. 3a,e). This phenomenon in electrochemical transistors was first exploited to demonstrate basic short-term synaptic plasticity functions, such as short-term depression, adaptation and dynamic filtering in a PEDOT:PSS (poly(3,4-ethylenedioxythiophene) polystyrene sulfonate)-based device<sup>47</sup>. Consequently, the device’s state retention was based on the slow kinetics of ionic movement from the conducting polymer film back into the electrolyte, and is thus considered volatile. Later, by slightly modifying the organic materials<sup>85</sup>, certain non-volatile behaviour, resulting from structural rearrangement of the polymer was also reported<sup>68</sup>.

Using a specific biasing scheme, researchers induced a non-volatile memory effect for a few hours, in a similar organic electrochemical transistor<sup>45</sup>. More recently, the addition of a ferroelectric layer was demonstrated to have a long-lasting memory effect<sup>86</sup>, common for ferroelectric materials<sup>33</sup>. In a polyaniline-based memristive device, the retention time was increased to about  $10^3$  s while simultaneously increasing switching rates by reducing the length of the conductive channel<sup>87</sup>. Physically limiting the movement of ions involved in the redox process was also reported to increase the retention time<sup>67</sup>. In this case, however, the resulting films remain in an electrochemically metastable state because the ionic charges are effectively stuck in the polymer due to drift/diffusion disparity between the anions and cations.

For long-term retention, it is more suitable to ensure electrical neutrality throughout the films in the device. This can be achieved by allowing a counter-redox reaction and was demonstrated in a two-terminal device with ethylviologen diperchlorate within a solid polyethylene-oxide electrolyte on top of a triphenylamine-containing polymer<sup>54</sup>. The cation in the solid electrolyte of this device can uptake an electron, while in the polymer side an electron is removed, which opens up a mobile hole (Fig. 3b,f). This device can essentially be considered as an electrochemical battery with two redox systems and mobile ions compensating for space-charge. The disadvantage of a two-terminal configuration, however, is that any pulse between the top and bottom electrodes, either write or read, results in bias through the complete redox system, thereby disturbing it. Thus, despite being electrically neutral, the reported device still lacks a high state stability; that is, it is volatile to a read operation.

In a similar configuration, but instead comprising a three-terminal configuration and polythiophene as the conducting polymer, researchers separated the read and write circuits to decouple the redox reactions during conductance tuning (write) (Fig. 3c,f) from the conduction state measurement (read) (Fig. 3c,g) in the polymer film<sup>48</sup>, thereby demonstrating enhanced two-state stability<sup>33</sup>. Although the conductivity modulation decreased marginally over time, it was still possible to distinguish between the two states. This modulation was thought to be the result of recombination reactions at the interface between the two sides of the redox system (orange dashed line in Fig. 3g). In fact, by adding a charge separation layer between the two sides, thus forming a device resembling an electrochemical battery that includes an electrolyte allowing only ion motion, it was possible to prevent interface recombination reactions and thus enhance state-retention for multiple states<sup>52</sup> (Fig. 3d,g).

As demonstrated in the previous sections, the electrochemical doping of conducting polymers allows for accurate tuning through a large range of oxidation and reduction states. However, a further reduced polymer is more susceptible to oxygen doping and consequently returns to an oxidized state. This inherently limits state-retention in semiconducting polymers but could be prevented by appropriate encapsulation, which reduces the effect of oxygen doping, or appropriate level tuning to stabilize the reduced polymer.

Charge-trapping is also an inherently metastable mechanism. However, the first reported neuromorphic devices based on charge-trapping already displayed a retention time of more than  $10^3$  s (ref. 55). The main difference with conventional floating-gate transistors is that the gold nanoparticles are inside the polymeric channel (that

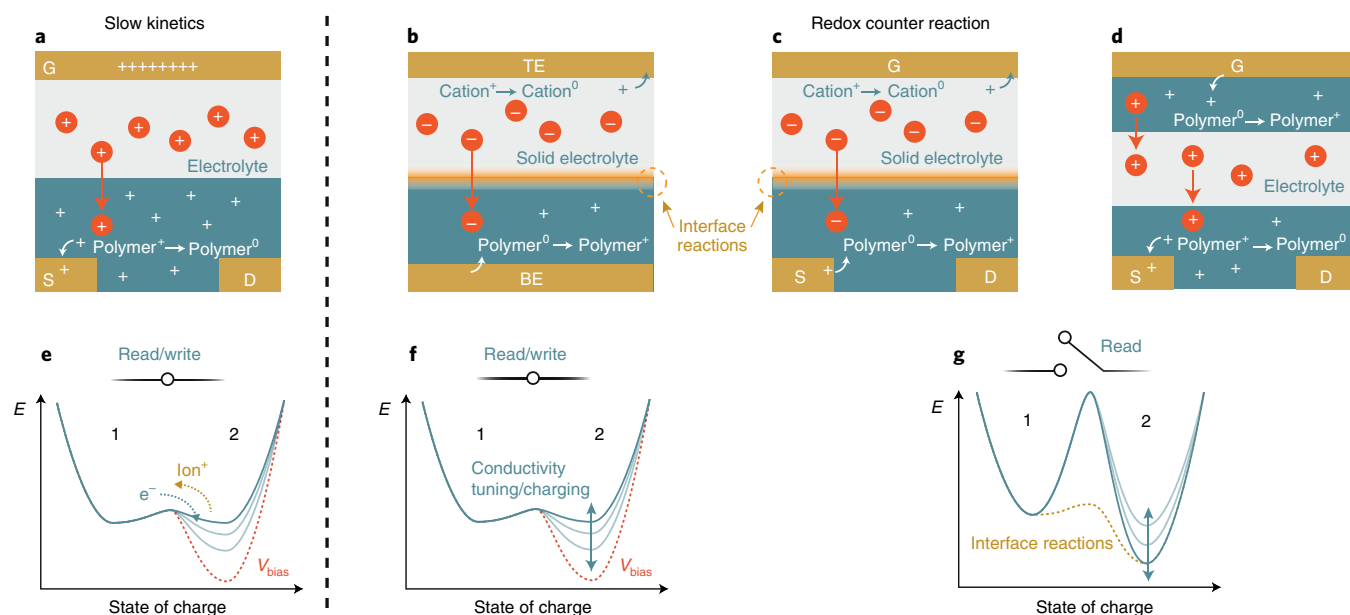


**Fig. 3 | Non-volatility in electrolyte-gated redox-based neuromorphic devices.** **a**, Electrochemical transistor-based devices rely on slow kinetics to retain a conductance state. **b–d**, Counter-redox reaction-based devices rely on a counter reaction in either the electrolyte in a two-terminal configuration (**b**), the three-terminal gated configuration (**c**) or comprising a conducting polymeric gate (**d**) to ensure electrical neutrality and thus enhance state retention. **e–g**, Related energy versus the state of charge. **e**, In electrochemical transistors a bias will change the electrochemical potential of the polymer films (dashed red lines in **e** and **f**) but offers little stability due to the low energy barrier for self-discharge. **f**, In two-terminal counter-redox-reaction-based mechanisms depicted in **b**, the write and the subsequent read action is similar to conventional electrochemical transistors, but state-retention is enhanced when no voltage is applied. **g**, Interface reactions can introduce local self-discharge. In three-terminal gated electrochemical devices (**c** and **d**), the read action is decoupled from the write action (similar to **f**) which prevents self-discharge via a large energetic barrier (**g**). However, without appropriate separation of the electrodes involved in the redox reaction, for example by an electrolyte, undesired interface reactions (dashed orange line) lower the barrier for local self-discharging.

is, the electronic charge conduction path is through the film with the particles), which limits the state stability and state-retention of these charge-trapping devices. By using a monolayer of functionalized gold nanoparticles, however, the researchers were able to demonstrate a higher retention of up to  $10^5$  s (ref. <sup>66</sup>).

**Cycling endurance.** For neuromorphic arrays to be useful for prolonged periods, it is important to study whether device performance deteriorates over time, for example during extensive read–write cycling. However, these characteristics have not been fully established, and the endurance requirements are not yet clear. For example, in flash memory devices  $\sim 10^4$  cycles are common, whereas static and dynamic random-access memory can be cycled over  $10^{16}$  times<sup>13</sup>. To investigate device performance, endurance measurements are usually done by cycling between adjacent conductance states or over the complete dynamic range. Although not many studies on organic neuromorphic devices include complete endurance cycling (that is, until failure), successful cycling has been demonstrated, ranging from 20 cycles in two-terminal memristive devices<sup>72</sup> up to 800 cycles in charge-trapping devices<sup>66</sup>. Redox-gated architectures were demonstrated from 50 cycles in early work<sup>88</sup> up to 10,000 cycles more recently<sup>87</sup> (Table 2). The optical memory-based device, on the other hand, showed state-retention times of up to  $10^7$  s with nearly no deterioration after 70 cycles<sup>73</sup>. These preliminary results show great promise for the long-term operation of neuromorphic devices and suggest that there is no intrinsic obstacle to achieving organic devices with high cycling endurance.

**Energy consumption.** In many devices energy consumption per synaptic or switching event is closely linked with read stability. In fact, the read stability of two-terminal devices is inherently linked to the energy needed to write or erase a state: low switching energies result in reduced stability, since a reading operation of a state can

disrupt the state itself. This trade-off is commonly circumvented by using a lower voltage to read a state and a higher voltage or current to write to a new state. Conventional inorganic memristive devices have reported writing energies of the order of 0.1–1,000 pJ (refs <sup>13,21</sup>) with typical device dimensions of 0.1–5  $\mu\text{m}$ , depending on the specific mechanisms and materials. Ultimately, the switching energy should be below 1 pJ to be competitive with traditional complementary metal–oxide–semiconductor (CMOS) logic circuits<sup>23</sup>.

Energy losses in the electrode lines leading to the devices in an array should also be taken into account. What this means is that a device located in the centre of an array should receive a certain minimum voltage, which may be relatively high, depending on the switching mechanism. Additional resistive losses in the electrode lines leading to that device may cause significantly higher energy costs<sup>13</sup>. For most filament-forming resistive-switching devices, a large energy difference between potentiation and depression is observed, owing to the high resetting current that is required. This was also the case for a reported polymer-based filament-forming resistive-switching mechanism, which required an energy of 0.1–100 pJ to switch, depending on the pulse number and whether it was lowering or enhancing the conductance<sup>89</sup>.

Redox coupling in polymeric materials is inherently a low-activation-energy process in which the voids between polymer chains — the free volume — facilitate the energetically cheap and reversible ion exchange, and thus enable low-energy switching. As a result, the energy for a single spiking operation resulting in a short-term modulation was found to be in the range of 10 pJ for a  $\sim 50 \mu\text{m}^2$  device<sup>67</sup>. For a complete write-read-erase operation of a  $100 \text{ nm} \times 100 \text{ nm}$  polymer device, the energy was estimated to be less than 10 pJ (ref. <sup>53</sup>).

In an effort to demonstrate ever-decreasing switching energies, a hybrid organic–inorganic perovskite memristive device was recently described with switching energies of the order of

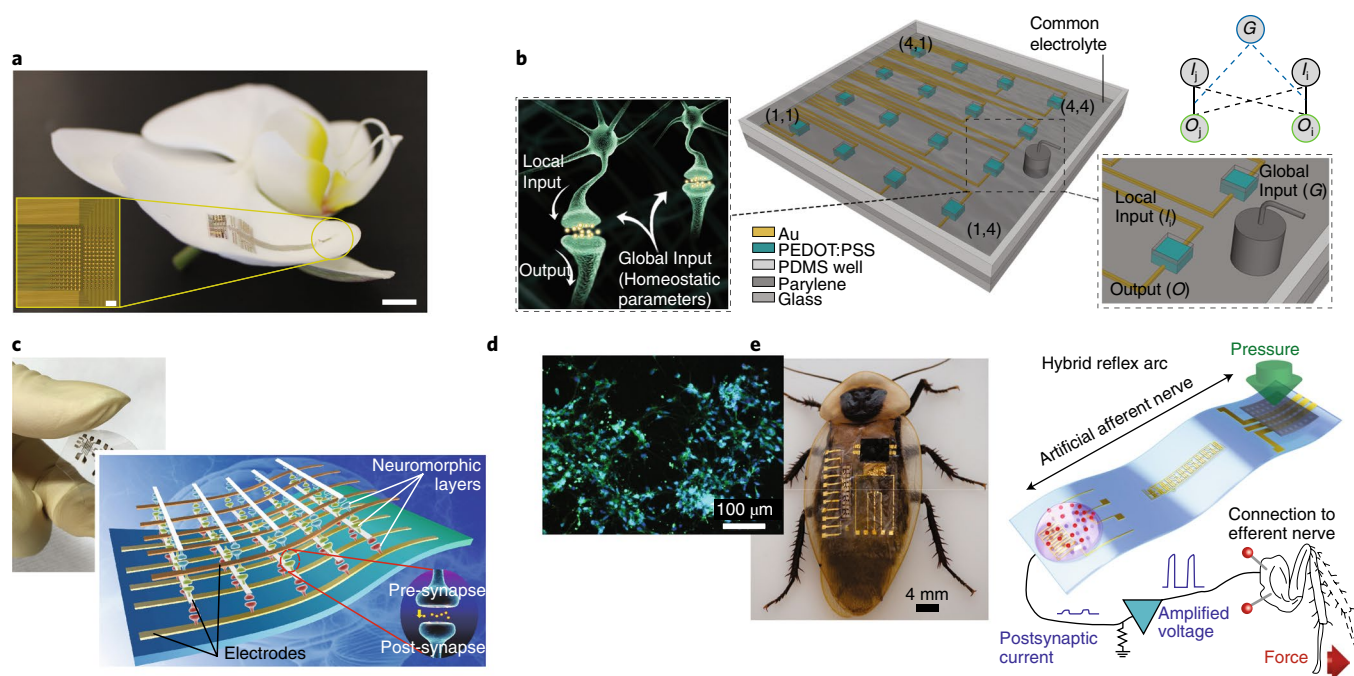


**Fig. 4 | Examples of integration and functionality.** **a**, A flexible organic-electronics-based implant structure conforms to the surface of an orchid petal (scale bar, 5 mm). Inset: optical micrograph of a 256-electrode NeuroGrid (scale bar, 100  $\mu\text{m}$ ). PEDOT:PSS covered electrodes are 10  $\mu\text{m}$   $\times$  10  $\mu\text{m}$ . **b**, Global gate induced effects on an organic neuromorphic device array. **c**, Three-dimensional flexible synaptic array. **d**, Neurons on top of an organic memristive device array. **e**, Artificial flexible afferent nerve connected to biological nerves in a cockroach. PDMS, Polydimethylsiloxane. Credit: reproduced from ref. <sup>105</sup>, Springer Nature Ltd (**a**); ref. <sup>103</sup>, Springer Nature Ltd (**b**); ref. <sup>89</sup>, Springer Nature Ltd (**c**); ref. <sup>79</sup>, Elsevier (**d**); and ref. <sup>109</sup>, AAAS (**e**)

femtojoules per 100  $\text{nm}^2$  (ref. <sup>90</sup>), which is comparable to the 10 fJ per synaptic event in the brain<sup>21</sup>. These low values are generally closely correlated with a lower state stability, as a low switching energy implies a switching process close to reversibility. In such conditions, slow ion kinetics are expected to result ultimately in a return to the original state, but this remains to be investigated explicitly.

In a battery-like artificial synapse with a higher state stability, the minimum energy needed to switch a 1,000  $\mu\text{m}^2$  device reliably was measured to be less than 10 pJ when the voltage source was tuned to the open-circuit potential of the device using a potentiostat. The energy was also found to scale with channel area, leading to an estimated absolute minimum switching energy of 35 aJ for a 300 nm  $\times$  300 nm device<sup>52</sup>. The large difference in energy when compared with other approaches might originate from the fact that in a battery-like artificial synapse, changing state requires the capacitor to be charged only slightly, which does not require much current. Furthermore, enhanced state-retention has the advantage that it enables the definition of distinct conductance states with a smaller difference in conductance than in the case of poor state-retention (large difference in conductance).

Charge-trapping devices traditionally operate with relatively high voltages ( $\sim 10$ – $40$  V) and consequently display high switching energies, although some examples of two-terminal bi-stable organic memory devices exist that operate with lower voltages of 3–5 V (refs <sup>91,92</sup>). More recently it was demonstrated that by optimizing the fabrication process of a nanoparticle organic memory field-effect transistor, the voltage required to switch was lowered to 1 V and the related energy could be reduced to 2 nJ (ref. <sup>93</sup>).

Further reducing the size of organic devices was also proven to decrease the necessary programming energy significantly, down to  $\sim 1$  fJ for an electrolyte-gated polyethylene oxide nanowire — the lowest value reported to date<sup>51</sup>. As such, organic neuromorphic devices have demonstrated great potential in enabling low switching energy, which is an essential characteristic of future low-power

neuromorphic computing. However, although low-power devices are highly desirable, the energy required to operate the complete neuromorphic system is the most relevant metric; for example, a low-power device that cannot be implemented in an energy-efficient neuromorphic system is not useful. Therefore, when developing single devices, their integration into and the efficiency of the final neuromorphic system must be carefully considered.

### Integration and biocompatibility

One common issue with organic electronics is that the large-scale integration of devices into useful applications may suffer from low device reproducibility and relatively low yield. However, a growing number of successful implementations of integrated devices are being demonstrated. Yang et al. reported the large-scale integration of organic neuromorphic devices, such as those previously demonstrated in flexible organic memory arrays<sup>81</sup>, in a flexible 3D network configuration<sup>89</sup> (Fig. 4c). This network consisted of three stacked copper-doped polymeric layers acting as a non-volatile memory array. In single artificial synapses coupled with a selector device, correlated learning following a spike-timing-dependent plasticity mechanism was demonstrated. Another integrated network was created by phase separation of block co-polymers<sup>94</sup>. Here, the authors were able to potentiate and depress an organic film simultaneously by creating separate conductance paths in three dimensions, effectively self-forming two memristive devices on a crossbar-point between four electrodes.

Apart from large (crossbar) arrays, several implementations of functional organic neuromorphic circuits have been reported, such as a single-layer perceptron consisting of two<sup>95</sup> or three<sup>69</sup> organic neuromorphic devices that could classify inputs via supervised learning. A perceptron emulates biological neuron functionality by summing and mapping the input signals to the output signal<sup>96</sup>. The two-device architecture also included the activation function based on an organic field-effect transistor and two organic resistors<sup>95</sup>, but training of the



memristive devices was done offline. In contrast, on-chip training was implemented to perform NAND and NOR functionality using simple threshold currents<sup>69</sup> as well as more complex circuitry combining organic memristive devices with CMOS-based neurons<sup>97</sup>. More elementary learning functionality, such as simple associative learning (for example, Pavlov's dog), has also been reported<sup>52,70,95,98,99</sup>.

An important feature of organic redox-based neuromorphic devices is the electrolyte, which allows novel architectures to be designed. One example is an architecture comprising one channel and multiple gates. The spatiotemporal coupling of applied signals to the gates controls the state of the channel. Using this concept, information processing functions (for example, orientation selectivity) inspired by the mammalian visual system were demonstrated<sup>100,101</sup> and later mimicked in a different polymer<sup>102</sup>. The electrolyte can also be used to couple one gate to multiple channels, in a way that is reminiscent of the global control of neurons in the brain, achieved by parameters such as hormones, ion concentration and temperature<sup>103</sup> (Fig. 4b). This property can be useful in large device arrays where a common bias is necessary. Other, more general, integrated ionic-based logic gates such as inverters and NAND gates can be potentially useful for integration with organic neuromorphic circuitry<sup>104</sup>.

Furthermore, the soft mechanics and biocompatibility of organic materials renders organic memristive elements and arrays highly appealing for interfacing with biology (Fig. 4a,d). Such interfacing has been demonstrated across a wide variety of applications, such as implants<sup>105,106</sup> (Fig. 4a), biosensors<sup>84</sup> and biomimetics<sup>107</sup>, as well as bio-inspired and biomaterials-based memories<sup>108</sup>. At the same time, the observation of short-term potentiation and synaptic operation in organic memristive arrays shows that these devices could operate with biological cells placed on top of the array<sup>79</sup> (Fig. 4d). Recently, organic ion gel-gated transistors were used in a flexible organic artificial afferent nerve to detect movement and pressure for use in neurorobotics and neuroprosthetics<sup>109</sup> (Fig. 4e). Additional development could further enhance the connection between synaptic memristive arrays and adaptive control of physiology and processes of cells, tissue and organs; and vice versa to enhance site-specific sensing and monitoring<sup>106,110</sup>.

Despite some progress in the integration of organic neuromorphic devices, several challenges remain to be tackled before large-scale programmable and functional neuromorphic arrays can be realized. Although the activation function, which implements biological neuron functionality, has been emulated by organic field-effect transistors<sup>95</sup>, it is not yet well-established how this functionality will be implemented in large-scale arrays with multiple hidden layers. Furthermore, sneak currents and voltages (unwanted conducting paths) through crossbar-array-based networks are common problems that require solutions in the form of rectifying behaviours inside the materials or additionally integrated access devices<sup>75</sup>, such as in dot-product engines<sup>12</sup>, to prevent undesirable device cross-talk.

## Outlook

Organic materials have the potential to be exploited successfully in neuromorphic computing owing to their low-energy switching, excellent tunability, low cost and biocompatibility. Specifically, access to a large conductance range and corresponding number of states is highly attractive for hardware-based forward-inference neural networks and related vector-matrix multiplication, which could enable fully parallel read and write neural algorithm accelerators. Furthermore, the ability to tailor the electrical, chemical and mechanical characteristics of organic compounds could allow for the development of near-ideal materials that possess long-term stability, linear switching characteristics and ability to switch at low energies, all while enabling integration in various form factors.

Despite recent successes, more research is necessary to overcome current limitations before organic neuromorphic devices can succeed. Read and write noise should be sufficiently reduced and state-retention further increased, especially for long-term operation. Encapsulation could help increase device stability and cycling endurance to desired levels.

While device-to-device variability remains an issue during fabrication, improvements are expected from high-quality manufacturing facilities. Yet apart from a few recent successful demonstrations of large-scale integration, organic neuromorphic arrays might suffer from low device reproducibility (particularly for devices downsized to less than 1  $\mu\text{m}^2$ ) and consequently array failure. This requires further investigation and development. Nevertheless, the large conductance range of redox-coupled devices can be used to determine an acceptable but reduced range for a large number of inferior devices that are fabricated in the same array. Combined with linear symmetric switching<sup>111</sup>, this could provide sufficient array performance.

Other essential functionality such as the activation function and related mapping of the input signals to output signals is still lacking — the path towards an efficient all-organic neuromorphic system is not yet clear. Eventually, it is very likely to be important that organic tunable memristive elements can also be integrated in inorganic or other conventional CMOS applications in order to broaden their appeal and adaptability. For instance, compact organic neuromorphic cores can be built into a digital CMOS processing unit to perform the most intensive vector-matrix operations, while communication between the neural cores would be executed by the digital CMOS processing units. Further integration into 'back end of the line' processing (for example, requiring materials to withstand elevated temperatures of ~350–400 °C) would have to be investigated and devised. An efficient organic-inorganic neuromorphic system that leverages the advantages of both technologies could serve as motivation for this pursuit. At the same time, switching mechanisms in organic devices can also serve as inspiration for inorganic devices, as was recently demonstrated in an Li-ion-based inorganic synapse for analogue computing<sup>112</sup>. In applications where dedicated local functionality and low energy are important, organic electronic materials can be highly complementary to inorganic CMOS-based neuromorphic arrays.

Finally, switching speed, which is essential during the training phase, is not well understood. The fundamental device mechanisms and their dependence on the nature of the materials used must be investigated in order to determine what limits switching speed and how it can be improved. An accurate physical model of these devices, which is extremely useful in this respect, is still missing. Such a model would also allow researchers to simulate accurately the complete behaviour of arrays of devices, thus greatly accelerating design feedback loops.

More exotic weight update mechanisms, such as those based on optically adjusting the weights<sup>74</sup>, could make organic neuromorphic devices unique compared with other technologies. This has a number of advantages, including the elimination of sneak currents, as mentioned earlier. Other unique properties of organic electronic materials, such as low-temperature processing and ink-jet manufacturing capabilities, could potentially enable low-cost, disposable and simple neuromorphic-based lab-on-chips, which could be utilized for smart point-of-care devices. We speculate that developments in organic neuromorphic computing could lead to and be exploited for enhanced hybrid biological/organic functionality such as trainable and adaptable brain-machine interfaces<sup>106</sup>, biosensor networks, robotic skin<sup>113</sup> and adaptable local control of prosthetics<sup>109</sup>.

Received: 20 February 2018; Accepted: 16 June 2018;  
Published online: 13 July 2018

## References

- Abbott, L. F. & Regehr, W. G. Synaptic computation. *Nature* **431**, 796–803 (2004).
- Hebb, D. O. *The Organization of Behavior: A Neuropsychological Theory*. (Wiley, New York, 1949).
- Mead, C. Neuromorphic electronic systems. *Proc. IEEE* **78**, 1629–1636 (1990). **This article contains the first mention of the term neuromorphic systems.**
- Indiveri, G. et al. Neuromorphic silicon neuron circuits. *Front. Neurosci.* **5**, 73 (2011).
- Qiao, N. et al. A reconfigurable on-line learning spiking neuromorphic processor comprising 256 neurons and 128K synapses. *Front. Neurosci.* **9**, 141 (2015).
- Burr, G. W. et al. Neuromorphic computing using non-volatile memory. *Adv. Phys. X* **2**, 89–124 (2017).
- Merolla, P. A. et al. A million spiking-neuron integrated circuit with a scalable communication network and interface. *Science* **345**, 668–673 (2014).
- Benjamin, B. V. et al. Neurogrid: A mixed-analog-digital multichip system for large-scale neural simulations. *Proc. IEEE* **102**, 699–716 (2014).
- Davies, M. et al. Loihi: A neuromorphic manycore processor with on-chip learning. *IEEE Micro* **38**, 82–99 (2018).
- Chua, L. O. Memristor — The missing circuit element. *IEEE T. Circuit Theory* **18**, 507–519 (1971). **This article reports the first theoretical description of the memristor.**
- Strukov, D. B., Snider, G. S., Stewart, D. R. & Williams, R. S. The missing memristor found. *Nature* **453**, 80–83 (2008).
- Miao, H. et al. Memristor-based analog computation and neural network classification with a dot product engine. *Adv. Mater.* **30**, 1705914 (2018).
- Yang, J. J., Strukov, D. B. & Stewart, D. R. Memristive devices for computing. *Nat. Nanotech.* **8**, 13–24 (2013).
- Simmons, J. G. & Verderber, R. R. New thin-film resistive memory. *Radio Electron. Eng.* **34**, 81–89 (1967). **This article reports the first experimental demonstration of a non-volatile analogue memory.**
- Oxley, D. P. Electroforming, switching and memory effects in oxide thin films. *Electro. Sci. Tech.* **3**, 217–224 (1977).
- Swaroop, B., West, W. C., Martinez, G., Kozicki, M. N. & Akers, L. A. Programmable current mode Hebbian learning neural network using programmable metallization cell. *Proc. 1998 IEEE Int. Symp. Circuits Syst.* **3**, 33–36 (1998).
- Alibart, F., Zamanidoost, E. & Strukov, D. B. Pattern classification by memristive crossbar circuits using ex situ and in situ training. *Nat. Commun.* **4**, 2072 (2013).
- Prezioso, M. et al. Training and operation of an integrated neuromorphic network based on metal-oxide memristors. *Nature* **521**, 61–64 (2015).
- Chang, T., Jo, S.-H. & Lu, W. Short-term memory to long-term memory transition in a nanoscale memristor. *ACS Nano* **5**, 7669–7676 (2011).
- Wang, Z. et al. Memristors with diffusive dynamics as synaptic emulators for neuromorphic computing. *Nat. Mater.* **16**, 101–108 (2017).
- Kuzum, D., Yu, S. & Wong, H.-S. P. Synaptic electronics: materials, devices and applications. *Nanotechnology* **24**, 382001 (2013).
- Agarwal, S. et al. Resistive memory device requirements for a neural algorithm accelerator. in *2016 Int. Joint Conf. Neural Networks* 929–938 (2016).
- Jeong, D. S., Kim, K. M., Kim, S., Choi, B. J. & Hwang, C. S. Memristors for energy-efficient new computing paradigms. *Adv. Electron. Mater.* **2**, 1600090 (2016).
- Someya, T., Bao, Z. & Malliaras, G. G. The rise of plastic bioelectronics. *Nature* **540**, 379–385 (2016).
- Gregor, L. V. Electrical conductivity of polydivinylbenzene films. *Thin Solid Films* **2**, 235–246 (1968).
- Carchano, H., Lacoste, R. & Segui, Y. Bistable electrical switching in polymer thin films. *Appl. Phys. Lett.* **19**, 414–415 (1971).
- Potember, R. S., Poehler, T. O. & Cowan, D. O. Electrical switching and memory phenomena in Cu-TCNQ thin films. *Appl. Phys. Lett.* **34**, 405–407 (1979).
- Gao, H. J. et al. Reversible, nanometer-scale conductance transitions in an organic complex. *Phys. Rev. Lett.* **84**, 1780–1783 (2000).
- Ma, L. P., Liu, J. & Yang, Y. Organic electrical bistable devices and rewritable memory cells. *Appl. Phys. Lett.* **80**, 2997–2999 (2002).
- Ma, L., Xu, Q. & Yang, Y. Organic nonvolatile memory by controlling the dynamic copper-ion concentration within organic layer. *Appl. Phys. Lett.* **84**, 4908–4910 (2004).
- Henisch, H. K. & Smith, W. R. Switching in organic polymer films. *Appl. Phys. Lett.* **24**, 589–591 (1974).
- Tondelier, D., Lmimouni, K., Vuillaume, D., Fery, C. & Haas, G. Metal/organic/metal bistable memory devices. *Appl. Phys. Lett.* **85**, 5763–5765 (2004).
- Asadi, K., de Leeuw, D. M., de Boer, B. & Blom, P. W. M. Organic non-volatile memories from ferroelectric phase-separated blends. *Nat. Mater.* **7**, 547–550 (2008).
- Naber, R. C. G., Asadi, K., Blom, P. W. M., de Leeuw, D. M. & de Boer, B. Organic nonvolatile memory devices based on ferroelectricity. *Adv. Mater.* **22**, 933–945 (2010).
- Kamitsos, E. I., Tzini, C. H. & Risen, W. M. Raman study of the mechanism of electrical switching in Cu TCNQ films. *Solid State Commun.* **42**, 561–565 (1982).
- Scott, J. C. & Bozano, L. D. Nonvolatile memory elements based on organic materials. *Adv. Mater.* **19**, 1452–1463 (2007).
- Ling, Q.-D. et al. Polymer electronic memories: Materials, devices and mechanisms. *Prog. Polym. Sci.* **33**, 917–978 (2008).
- Heremans, P. et al. Polymer and organic nonvolatile memory devices. *Chem. Mater.* **23**, 341–358 (2011).
- Cho, B., Song, S., Ji, Y., Kim, T.-W. & Lee, T. Organic resistive memory devices: Performance enhancement, integration, and advanced architectures. *Adv. Funct. Mater.* **21**, 2806–2829 (2011).
- Yu, S. et al. Stochastic learning in oxide binary synaptic device for neuromorphic computing. *Front. Neurosci.* **7**, 186 (2013).
- Shibata, T. & Ohmi, T. Neural microelectronics. in *Int. Electron. Dev. Meet. Tech. Digest* 337–342 (1997).
- Jo, S. H. et al. Nanoscale memristor device as synapse in neuromorphic systems. *Nano Lett.* **10**, 1297–1301 (2010).
- Möller, S., Perlov, C., Jackson, W., Taussig, C. & Forrest, S. R. A polymer/semiconductor write-once read-many-times memory. *Nature* **426**, 166–169 (2003).
- Kaneto, K., Asano, T. & Takashima, W. Memory device using a conducting polymer and solid polymer electrolyte. *Jpn J. Appl. Phys.* **30**, L215–L217 (1991). **This article reports the first demonstration of hybrid electronic/ionic switching in a conducting-polymer-based non-volatile memory device.**
- Nilsson, D. et al. Bi-stable and dynamic current modulation in electrochemical organic transistors. *Adv. Mater.* **14**, 51–54 (2002).
- Erokhin, V., Berzina, T. & Fontana, M. P. Hybrid electronic device based on polyaniline-polyethyleneoxide junction. *J. Appl. Phys.* **97**, 064501 (2005).
- Gkoupidenis, P., Schaefer, N., Garlan, B. & Malliaras, G. G. Neuromorphic functions in PEDOT:PSS organic electrochemical transistors. *Adv. Mater.* **27**, 7176–7180 (2015). **This article demonstrates synaptic functionality in an electrochemically gated conducting polymer device.**
- Kumar, R., Pillai, R. G., Pekas, N., Wu, Y. & McCreery, R. L. Spatially resolved Raman spectroelectrochemistry of solid-state polythiophene/viologen memory devices. *J. Am. Chem. Soc.* **134**, 14869–14876 (2012).
- Qian, C. et al. Artificial synapses based on in-plane gate organic electrochemical transistors. *ACS Appl. Mater. Inter.* **8**, 26169–26175 (2016).
- Kong, L. et al. Long-term synaptic plasticity simulated in ionic liquid/polymer hybrid electrolyte gated organic transistors. *Org. Electron.* **47**, 126–132 (2017).
- Xu, W., Min, S.-Y., Hwang, H. & Lee, T.-W. Organic core-sheath nanowire artificial synapses with femtojoule energy consumption. *Sci. Adv.* **2**, e1501326 (2016). **This article shows an artificial synapse that switches at femtojoule energy consumption.**
- van de Burgt, Y. et al. A non-volatile organic electrochemical device as a low-voltage artificial synapse for neuromorphic computing. *Nat. Mater.* **16**, 414–418 (2017).
- Das, B. C., Szeto, B., James, D. D., Wu, Y. & McCreery, R. L. Ion transport and switching speed in redox-gated 3-terminal organic memory devices. *J. Electrochem. Soc.* **161**, H831–H838 (2014).
- Liu, G. et al. Organic biomimicking memristor for information storage and processing applications. *Adv. Electron. Mater.* **2**, 1500298 (2016).
- Novembre, C., Guérin, D., Lmimouni, K., Gamrat, C. & Vuillaume, D. Gold nanoparticle-pentacene memory transistors. *Appl. Phys. Lett.* **92**, 103314 (2008).
- Ouyang, J., Chu, C.-W., Szmanda, C. R., Ma, L. & Yang, Y. Programmable polymer thin film and non-volatile memory device. *Nat. Mater.* **3**, 918–922 (2004). **This article demonstrates the first solution-processed bistable organic memory device based on charge storage.**
- Bozano, L. D., Kean, B. W., Deline, V. R., Salem, J. R. & Scott, J. C. Mechanism for bistability in organic memory elements. *Appl. Phys. Lett.* **84**, 607–609 (2004).
- Son, D. I., You, C. H., Kim, W. T., Jung, J. H. & Kim, T. W. Electrical bistabilities and memory mechanisms of organic bistable devices based on colloidal ZnO quantum dot-polymethylmethacrylate polymer nanocomposites. *Appl. Phys. Lett.* **94**, 132103 (2009).

59. Zhou, Y., Han, S., Sonar, P. & Roy, V. A. L. Nonvolatile multilevel data storage memory device from controlled ambipolar charge trapping mechanism. *Sci. Rep.* **3**, 2319 (2013).
  60. Kim, C.-H., Sung, S. & Yoon, M.-H. Synaptic organic transistors with a vacuum-deposited charge-trapping nanosheet. *Sci. Rep.* **6**, srep33355 (2016).
  61. Alibart, F. et al. An organic nanoparticle transistor behaving as a biological spiking synapse. *Adv. Funct. Mater.* **20**, 330–337 (2010).
  62. Alibart, F. et al. A memristive nanoparticle/organic hybrid synapstor for neuroinspired computing. *Adv. Funct. Mater.* **22**, 609–616 (2012).
  63. Valov, I. & Kozicki, M. Non-volatile memories: Organic memristors come of age. *Nat. Mater.* **16**, 1170–1172 (2017).
  64. Burr, G. W. et al. Phase change memory technology. *J. Vac. Sci. Technol. B* **28**, 223–262 (2010).
  65. Agarwal, S. et al. Designing an analog crossbar based neuromorphic accelerator. in *2017 5th Berkeley Symp. on Energy Efficient Electronic Systems Steep Transistors Workshop (E3S)* 1–3 (2017).
  66. Zhang, T. et al. Negative differential resistance, memory, and reconfigurable logic functions based on monolayer devices derived from gold nanoparticles functionalized with electropolymerizable TEDOT units. *J. Phys. Chem. C* **121**, 10131–10139 (2017).
  67. Lai, Q. et al. Ionic/electronic hybrid materials integrated in a synaptic transistor with signal processing and learning functions. *Adv. Mater.* **22**, 2448–2453 (2010).
  68. Gkoupidenis, P., Schaefer, N., Strakosas, X., Fairfield, J. A. & Malliaras, G. G. Synaptic plasticity functions in an organic electrochemical transistor. *Appl. Phys. Lett.* **107**, 263302 (2015).
  69. Demin, V. A. et al. Hardware elementary perceptron based on polyaniline memristive devices. *Org. Electron.* **25**, 16–20 (2015).
  70. Smerieri, A., Berzina, T., Erokhin, V. & Fontana, M. P. Polymeric electrochemical element for adaptive networks: Pulse mode. *J. Appl. Phys.* **104**, 114513 (2008).
  71. Xuan, Y., Sandberg, M., Berggren, M. & Crispin, X. An all-polymer-air PEDOT battery. *Org. Electron.* **13**, 632–637 (2012).
  72. Zeng, F., Li, S., Yang, J., Pan, F. & Guo, D. Learning processes modulated by the interface effects in a Ti/conducting polymer/Ti resistive switching cell. *RSC Adv.* **4**, 14822–14828 (2014).
  73. Leydecker, T. et al. Flexible non-volatile optical memory thin-film transistor device with over 256 distinct levels based on an organic bicomponent blend. *Nat. Nanotech.* **11**, 769–775 (2016).
  74. Tan, H. et al. Light-gated memristor with integrated logic and memory functions. *ACS Nano* **11**, 11298–11305 (2017).
  75. Burr, G. W. et al. Access devices for 3D crosspoint memory. *J. Vac. Sci. Technol. B* **32**, 040802 (2014).
  76. Rumelhart, D. E., Hinton, G. E. & Williams, R. J. Learning representations by back-propagating errors. *Nature* **323**, 533–536 (1986).
  77. Lapkin, D. A., Emelyanov, A. V., Demin, V. A., Berzina, T. S. & Erokhin, V. V. Spike-timing-dependent plasticity of polyaniline-based memristive element. *Microelectron. Eng.* **185–186**, 43–47 (2018).
  78. Li, S. Z. et al. Synaptic plasticity and learning behaviours mimicked through Ag interface movement in an Ag/conducting polymer/Ta memristive system. *J. Mater. Chem. C* **1**, 5292–5298 (2013).
  79. Desbief, S. et al. Electrolyte-gated organic synapse transistor interfaced with neurons. *Org. Electron.* **38**, 21–28 (2016).
  80. Ohno, T. et al. Short-term plasticity and long-term potentiation mimicked in single inorganic synapses. *Nat. Mater.* **10**, 591–595 (2011).
  81. Sekitani, T. et al. Organic nonvolatile memory transistors for flexible sensor arrays. *Science* **326**, 1516–1519 (2009).
  82. Nawrocki, R. A. et al. An inverted, organic WORM device based on PEDOT:PSS with very low turn-on voltage. *Org. Electron.* **15**, 1791–1798 (2014).
  83. Goswami, S. et al. Robust resistive memory devices using solution-processable metal-coordinated azo aromatics. *Nat. Mater.* **16**, 1216–1224 (2017).
  84. Rivnay, J. et al. Organic electrochemical transistors. *Nat. Rev. Mater.* **3**, 17086 (2018).
  85. Winther-Jensen, B., Kolodziejczyk, B. & Winther-Jensen, O. New one-pot poly(3,4-ethylenedioxythiophene): poly(tetrahydrofuran) memory material for facile fabrication of memory organic electrochemical transistors. *APL Mater.* **3**, 014903 (2014).
  86. Fabiano, S. et al. Ferroelectric polarization induces electronic nonlinearity in ion-doped conducting polymers. *Sci. Adv.* **3**, e1700345 (2017).
  87. Lapkin, D. A. et al. Polyaniline-based memristive microdevice with high switching rate and endurance. *Appl. Phys. Lett.* **112**, 043302 (2018).
  88. Erokhin, V., Berzina, T., Camorani, P. & Fontana, M. P. On the stability of polymeric electrochemical elements for adaptive networks. *Colloid Surf. A* **321**, 218–221 (2008).
  89. Wu, C., Kim, T. W., Choi, H. Y., Strukov, D. B. & Yang, J. J. Flexible three-dimensional artificial synapse networks with correlated learning and trainable memory capability. *Nat. Commun.* **8**, 752 (2017).
- This article demonstrates a three-dimensional integrated artificial synapse network.**
90. Xiao, Z. & Huang, J. Energy-efficient hybrid perovskite memristors and synaptic devices. *Adv. Electron. Mater.* **2**, 1600100 (2016).
  91. Kang, S. H., Crisp, T., Kymissis, I. & Bulović, V. Memory effect from charge trapping in layered organic structures. *Appl. Phys. Lett.* **85**, 4666–4668 (2004).
  92. Lin, H. T., Pei, Z. & Chan, Y. J. Carrier transport mechanism in a nanoparticle-incorporated organic bistable memory device. *IEEE Electron. Dev. Lett.* **28**, 569–571 (2007).
  93. Desbief, S. et al. Low voltage and time constant organic synapse-transistor. *Org. Electron.* **21**, 47–53 (2015).
  94. Erokhin, V. et al. Stochastic hybrid 3D matrix: Learning and adaptation of electrical properties. *J. Mater. Chem.* **22**, 22881–22887 (2012).
  95. Nawrocki, R. A., Voyles, R. M. & Shaheen, S. E. Neurons in polymer: Hardware neural units based on polymer memristive devices and polymer transistors. *IEEE T. Electron. Dev.* **61**, 3513–3519 (2014).
  96. Rosenblatt, F. The perceptron: A probabilistic model for information storage and organization in the brain. *Psychol. Rev.* **65**, 386–408 (1958).
  97. Lin, Y.-P. et al. Physical realization of a supervised learning system built with organic memristive synapses. *Sci. Rep.* **6**, 31932 (2016).
  98. Erokhin, V. et al. Material memristive device circuits with synaptic plasticity: Learning and memory. *BioNanoSci* **1**, 24–30 (2011).
  99. Bichler, O. et al. Pavlov's dog associative learning demonstrated on synaptic-like organic transistors. *Neural Comput.* **25**, 549–566 (2012).
  100. Gkoupidenis, P., Rezaei-Mazinani, S., Proctor, C. M., Ismailova, E. & Malliaras, G. G. Orientation selectivity with organic photodetectors and an organic electrochemical transistor. *AIP Adv.* **6**, 111307 (2016).
  101. Gkoupidenis, P., Koutsouras, D. A., Lonjaret, T., Fairfield, J. A. & Malliaras, G. G. Orientation selectivity in a multi-gated organic electrochemical transistor. *Sci. Rep.* **6**, 27007 (2016).
  102. Qian, C., Kong, L., Yang, J., Gao, Y. & Sun, J. Multi-gate organic neuron transistors for spatiotemporal information processing. *Appl. Phys. Lett.* **110**, 083302 (2017).
  103. Gkoupidenis, P., Koutsouras, D. A. & Malliaras, G. G. Neuromorphic device architectures with global connectivity through electrolyte gating. *Nat. Commun.* **8**, 15448 (2017).
  104. Tybrandt, K., Forchheimer, R. & Berggren, M. Logic gates based on ion transistors. *Nat. Commun.* **3**, 1869 (2012).
  105. Khodagholy, D. et al. NeuroGrid: Recording action potentials from the surface of the brain. *Nat. Neurosci.* **18**, 310–315 (2015).
  106. Rivnay, J., Wang, H., Fenno, L., Deisseroth, K. & Malliaras, G. G. Next-generation probes, particles, and proteins for neural interfacing. *Sci. Adv.* **3**, e1601649 (2017).
  107. Simon, D. T. et al. An organic electronic biomimetic neuron enables auto-regulated neuromodulation. *Biosens. Bioelectron.* **71**, 359–364 (2015).
  108. Lv, Z., Zhou, Y., Han, S.-T. & Roy, V. A. L. From biomaterial-based data storage to bio-inspired artificial synapse. *Mater. Today* <https://doi.org/10.1016/j.mattod.2017.12.001> (February 2018).
  109. Kim, Y. et al. A bioinspired flexible organic artificial afferent nerve. *Science* **360**, 998–1003 (2018).
  110. Simon, D. T., Gabrielsson, E. O., Tybrandt, K. & Berggren, M. Organic bioelectronics: Bridging the signaling gap between biology and technology. *Chem. Rev.* **116**, 13009–13041 (2016).
  111. Keene, S. T. et al. Optimized pulsed write schemes improve linearity and write speed for low-power organic neuromorphic devices. *J. Phys. D.* **51**, 224002 (2018).
  112. Fuller, E. J. et al. Li-ion synaptic transistor for low power analog computing. *Adv. Mater.* **29**, 1604310 (2016).
  113. Chortos, A., Liu, J. & Bao, Z. Pursuing prosthetic electronic skin. *Nat. Mater.* **15**, 937–950 (2016).
  114. Berzina, T. et al. Optimization of an organic memristor as an adaptive memory element. *J. Appl. Phys.* **105**, 124515 (2009).
  115. Krizhevsky, A., Sutskever, I. & Hinton, G. E. ImageNet classification with deep convolutional neural networks. in *Advances in Neural Information Processing Systems 25* (eds Pereira, F., Burges, C. J. C., Bottou, L. & Weinberger, K. Q.) 1097–1105 (Curran Associates, Red Hook, NY, 2012).
  116. Hinton, G. E., Osindero, S. & Teh, Y.-W. A fast learning algorithm for deep belief nets. *Neural Comput.* **18**, 1527–1554 (2006).
  117. Rumelhart, D. E. & McClelland, J. L., PDP Research Group. *Parallel Distributed Processing: Explorations in the Microstructure of Cognition, Vol. 1: Foundations* (MIT Press, Cambridge, MA, 1987).
  118. LeCun, Y., Bengio, Y. & Hinton, G. Deep learning. *Nature* **521**, 436–444 (2015).

**Acknowledgements**

The authors would like to thank M. Marinella and S. Agarwal from Sandia National Labs for help in preparing this document. A.M. gratefully acknowledges support from the Knut and Alice Wallenberg Foundation (KAW 2016.0494) for postdoctoral research at Stanford University. S.T.K. was funded by the Stanford Graduate Fellowship.

**Author contributions**

Y.v.d.B. collected all the articles and data. Y.v.d.B., A.M. and S.K. wrote the manuscript. All authors contributed to the discussion and writing.

**Competing interests**

The authors declare no competing interests.

**Additional information**

**Reprints and permissions information** is available at [www.nature.com/reprints](http://www.nature.com/reprints).

**Correspondence** should be addressed to Y.v.d.B. or A.M.

**Publisher's note:** Springer Nature remains neutral with regard to jurisdictional claims in published maps and institutional affiliations.